# Nonlinear effects in quasi-linear dispersion-managed pulse transmission

| | |
|---|---|
| 著者 | 廣岡　俊彦 |
| journal or publication title | IEEE Photinics Technology Letters |
| volume | 13 |
| number | 10 |
| page range | 1082-1084 |
| year | 2001 |
| URL | http://hdl.handle.net/10097/47734 |

doi: 10.1109/68.950742

# Nonlinear Effects in Quasi-Linear Dispersion-Managed Pulse Transmission

Mark J. Ablowitz and Toshihiko Hirooka, *Member, IEEE*

***Abstract*—The role of nonlinearity on quasi-linear pulse transmission in strongly dispersion-managed systems with loss and amplification is analyzed. The spectral characteristics of the pulse evolution are strongly dependent on the relative position of the amplifier in the dispersion map. The results agree well with direct numerical simulations and recent experiments.**

***Index Terms*—Dispersion management, optical fiber communication, optical fiber nonlinearity.**

In recent years return-to-zero (RZ) optical pulse transmission in strongly dispersion-managed fibers has become a crucial technology. By suitably employing strong dispersion management, researchers have been able to suppress certain nonlinear effects [1]. In this case, the RZ pulses are often referred to as quasi-linear RZ or chirped RZ (CRZ) pulses, as distinguished from solitons where nonlinearity balances dispersion. In this letter, we provide an analytical framework, which is effective in describing quasi-linear transmission in realistic strongly dispersion-managed systems with loss and amplification. The suppression of nonlinear effects is found to be dependent on large values of the map strength $s$ [a definition of map strength for two-step maps is given below (3)]. Indeed future systems with channel bit rates of 40 Gb/s and beyond may well depend on large values of map strength [2].

Based on our analysis for large map strengths, we find that the spectral structure of the pulse evolution depends significantly on the relative position of the lumped amplifiers within a dispersion map period. When the amplifiers are located at the discontinuity point of the dispersion map, the nonlinear phase shift in the frequency is found to preserve the spectral intensity in a manner similar to that found in the lossless case [3]. On the other hand, the nonlinearity is responsible for significant spectral reshaping when the amplifiers are positioned in the middle of the anomalous or normal dispersion segments. Our results compare favorably with direct numerical simulations and recent experimental observations [4]–[6].

The analysis begins with the nonlinear Schrödinger (NLS) equation in the presence of dispersion variation, loss, and lumped amplifcation. We introduce dimensionless variables $t = t_{\mathrm{ret}}/t_*$, $z = z_{\mathrm{lab}}/z_*$, $u = E/\sqrt{gP_*}$, and $d = k''/k''_*$ with characteristic parameters denoted by the subscript $*$, where $t_{\mathrm{ret}}$ and $z_{\mathrm{lab}}$ are the retarded time and the propagation distance, respectively, and $E$ denotes the slowly varying envelope of the optical field. With typical choices of $t_*$, $P_*$, and $z_* = z_{\mathrm{NL}} \equiv 1/\nu P_*$ with $\nu$ being the nonlinear coefficient (which yields $k''_* = -t_*^2/z_{\mathrm{NL}}$), we have the nondimensional perturbed NLS

$$i\frac{\partial u}{\partial z} + \frac{d(z)}{2}\frac{\partial^2 u}{\partial t^2} + g(z)|u|^2 u = 0. \qquad (1)$$

The functions $d(z)$ and $g(z)$ describe the dispersion variation of the fiber and the variation of power due to loss and lumped amplification, respectively, which are both periodic with period $z_a$, $z_a$ being the nondimensional amplifier distance which is assumed small ($z_a \ll 1$). As is standard, $g(z)$ is given by $g(\zeta) = 2G\exp(2G)\mathrm{csch}(2G)\exp[-4G(\zeta - n - \zeta_a)]$, $\zeta_a + n \le \zeta < \zeta_a + n + 1$, $g(0) = 2\Gamma z_a/[1-\exp(-2\Gamma z_a)]$, where $\zeta = z/z_a$, $G = \Gamma z_a/2$, and $\Gamma$ is the dimensionless loss coefficient. To model strong dispersion management, we assume that $d(z)$ takes the form $d(z) = \langle d\rangle + (1/z_a)\Delta(z/z_a)$ where the constant $\langle d\rangle$ represents the path-average dispersion and $\Delta(z/z_a)$ describes the rapid variation of group-velocity dispersion (GVD) with zero average. An appropriate multiscale expansion of the perturbed NLS equation yields the following averaged equation [7], referred to as dispersion-managed NLS (DMNLS) equation (see also [8]). In the frequency domain we have

$$i\frac{\partial \hat{U}}{\partial z} - \frac{\langle d\rangle}{2}\omega^2\hat{U} + \iint_{-\infty}^{\infty} d\omega_1 d\omega_2 \hat{U}(z,\omega+\omega_1)\hat{U}(z,\omega+\omega_2) \times \hat{U}^*(z,\omega+\omega_1+\omega_2) r(\omega_1\omega_2) = 0 \qquad (2)$$

where $\hat{u}(z,\omega) \sim \hat{U}(z,\omega)\exp[-iC(z/z_a)\omega^2/2]$, $\hat{u}(z,\omega) = \int_{-\infty}^{\infty} dt u(z,t)\exp(-i\omega t)$, and $C(\zeta) = C_0 + \int_0^\zeta d\zeta' \Delta(\zeta')$ with an arbitrary constant $C_0$. The kernel $r(\omega_1\omega_2)$ defined as

$$r(x) = \frac{1}{(2\pi)^2}\int_{-1/2}^{1/2} d\zeta\, g(\zeta)\exp[iC(\zeta)x] \qquad (3)$$

represents the structure of the map. In what follows we consider a symmetric two-step dispersion map as shown in Fig. 1, composed of fiber segments of equal length with positive and negative constant values of GVD $\Delta(z) = \pm\Delta$, respectively. The origin $\zeta = 0$ is fixed to be the middle point of an anomalous GVD segment with $C_0 = 0$ (the chirp-free point). It is convenient to introduce a parameter $s = (d - \langle d\rangle)z_a/4 = \Delta/4$ as a measure of the map strength of this profile. Note that the map strength is usually defined in terms of dimensional quantities $S = (4t_*^2/t_{\mathrm{FWHM}}^2)s$ [9]. We introduce a parameter $\zeta_a$ to describe the relative location of the amplifier within one dispersion map period. When $\zeta_a = 0$, the amplifiers are positioned

Manuscript received March 14, 2001; revised June 18, 2001. This work was supported in part by the National Science Foundation under Grant ECS-9800152, and by the Air Force Office of Scientific Research, Air Force Materials Command under Grant F49620-00-1-0031.

The authors are with the Department of Applied Mathematics, University of Colorado, Boulder, CO 80309-0526 USA (e-mail: hirooka@colorado.edu).

Publisher Item Identifier S 1041-1135(01)08134-4.

1041-1135/01$10.00 © 2001 IEEE

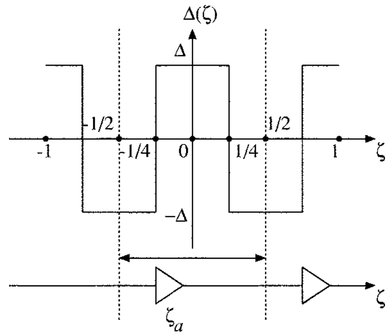


Fig. 1. Schematic diagram of two-step dispersion map.

in the middle of the anomalous GVD segment. From Fig. 1, we see that $\zeta_a$ can be restricted in the range $-1/2 \le \zeta_a < 1/2$.

We look for the asymptotic behavior of the nonlinear term in DMNLS equation for large map strength $s$ (see also [3] and [10] where lossless cases are discussed). The kernel $r(x;s)$ in the symmetric two-step dispersion map is obtained by a straightforward integration of (3). In a system including loss and lumped amplification (namely when $g(z) \neq 1$), the kernel $r(x)$ depends not only on $s$ but also on $\zeta_a$. In the following, we study four cases where amplifiers are positioned (i) in the middle of anomalous GVD segments ($\zeta_a = 0$), (ii) in the middle of normal GVD segments ($-1/2$), (iii) at the boundary between anomalous and normal GVD segments ($-1/4$), and (iv) at the boudary between normal and anomalous GVD segments ($1/4$).

When $\zeta_a = -1/4 \pm 1/4$ (i.e., $\zeta_a = 0$ and $-1/2$), from (3) the kernel is found to be

$$r(x;s) = \frac{1}{(2\pi)^2}\frac{G}{(sx)^2+G^2}\Big[sx\sin(sx)\operatorname{csch}G + G \pm isx\big(1-\cos(sx)\operatorname{sech}G\big)\Big]. \quad (4)$$

Assuming that $\hat{U}(z,\omega)$ depends only weakly on $s$, an asymptotic expansion of the nonlinear term in (2) for $s \gg 1$ yields

$$i\frac{\partial \hat{U}}{\partial z} - \frac{\langle d\rangle}{2}\omega^2\hat{U} + \frac{1}{s}(K_0\log s - K_1)\hat{J}_1(z,\omega) - \frac{K_0}{s}\hat{J}_2(z,\omega) \mp i\frac{K_2}{s}\hat{J}_3(z,\omega) = 0 \quad (5)$$

where

$$\hat{J}_1(z,\omega) = |\hat{U}(z,\omega)|^2\hat{U}(z,\omega) \quad (6a)$$

$$\hat{J}_2(z,\omega) = \hat{U}(z,\omega)\int_{-\infty}^{\infty} d\omega' |\hat{U}(z,\omega')|^2 h(\omega'-\omega) \quad (6b)$$

$$\hat{J}_3(z,\omega) = \int_{-\infty}^{\infty}\!\!\!\!\!\!\!\!-\;\;\int_{-\infty}^{\infty}\!\!\!\!\!\!\!\!-\;\;\frac{d\omega_1 d\omega_2}{\omega_1\omega_2}\hat{U}(z,\omega+\omega_1) \times \hat{U}(z,\omega+\omega_2)\hat{U}^*(z,\omega+\omega_1+\omega_2) \quad (6c)$$

and $h(\omega) = (1/\pi)\int_{-\infty}^{\infty} dt \log|t| \exp(-i\omega t)$. The constants $K_0$, $K_1$, and $K_2$ are defined as $K_0 = (G/2\pi)(\exp(-G)\operatorname{csch} G + 1)$, $K_1 = (G/4\pi)\operatorname{csch} G[\exp(G)I_{G1} + \exp(-G)(3\gamma + \log G - I_{G2})] + (G/2\pi)(2\gamma + \log G)$, and $K_2 = G/4$, where $I_{G1} = \int_G^\infty dx \exp(-x)/x$, $I_{G2} = \int_0^G dx(\exp(x)-1)/x$, and $\gamma = 0.577\,22$ is Euler's constant. In the limit of $G \to 0$, (5) reduces to the result obtained in [3] ($K_0 \to 1/2\pi$, $K_1 \to \gamma/2\pi$, and $K_2 \to 0$). From (5), the evolution of the intensity is described as

$$\frac{\partial|\hat{U}|^2}{\partial z} = \pm\frac{K_2}{s}f(z,\omega) \quad (7)$$

where $f(z,\omega) = \hat{J}_3(z,\omega)\hat{U}^*(z,\omega) + \hat{J}_3^*(z,\omega)\hat{U}(z,\omega)$. Since $s$ is large, the solution of (7) can be approximated by

$$|\hat{U}(z,\omega)|^2 \approx |\hat{U}(0,\omega)|^2 \pm \frac{K_2 z}{s}f(0,\omega) \quad (8)$$

for moderate values of $z$.

When $\zeta_a = \pm 1/4$, from (3) the kernel is found to be

$$r(x;s) = \frac{1}{(2\pi)^2}\frac{G}{(sx)^2+G^2} \times \Big\{\big(\exp(G)\operatorname{csch}G - 1\big)sx\sin(sx) + G\cos(sx) \pm i\Big[\big(\exp(-G)\operatorname{sech}G - 1\big) \times sx\cos(sx) + G\sin(sx)\Big]\Big\}. \quad (9)$$

In this case, (2) when $s \gg 1$ is written as

$$i\frac{\partial \hat{U}}{\partial z} - \frac{\langle d\rangle}{2}\omega^2\hat{U} + \frac{1}{s}(L_0\log s - L_1)\hat{J}_1(z,\omega) - \frac{L_0}{s}\hat{J}_2(z,\omega) = 0 \quad (10)$$

where the constants $L_0$ and $L_1$ are defined as $L_0 = (G/2\pi)\exp(-2G)\operatorname{csch}G$, $L_1 = (G\exp(-G)/4\pi)\operatorname{csch}G[\exp(G)I_{G1} + \exp(-G)(3\gamma + \log G - I_{G2})] - (G\exp(G)/2\pi)I_{G1}$. Neglecting $O(1/s^2)$ terms, we find from (10) that the spectral intensity $|\hat{U}(z,\omega)|^2$ is preserved during pulse propagation. Correspondingly, the solution of (2) is

$$\hat{U}(z,\omega) = \hat{U}(0,\omega)\exp\left\{-\frac{i\langle d\rangle\omega^2 z}{2} + i\Psi\left[|\hat{U}(0,\omega)|^2\right]z\right\} \quad (11a)$$

$$\Psi\left[|\hat{U}(z,\omega)|^2\right] = \frac{1}{s}\Big[(L_0\log s - L_1)|\hat{U}(z,\omega)|^2 - L_0\int_{-\infty}^{\infty} d\omega' h(\omega'-\omega)|\hat{U}(z,\omega')|^2\Big] \quad (11b)$$

where $h(\omega)$ is given above. After the linear phase shift $\exp(-i\langle d\rangle\omega^2 z/2)$ is removed by means of pre- or post-transmission compensation, the averaged dynamics of the quasi-linear pulse transmission is characterized only by the nonlinear phase shift $\phi_{\mathrm{NL}}(z,\omega) = \Psi[|\hat{U}(0,\omega)|^2]z$ as in the lossless limit $G \to 0$ [3] ($L_0 \to 1/2\pi$ and $L_1 \to \gamma/2\pi$).

In order to test the above analysis, we compared our results with direct numerical simulations of (1) with $\langle d\rangle = 0$, $\Gamma = 10$, and $z_a = 0.1$ (namely $G = 0.5$). The incident pulse is given by a Gaussian $u(0,t) = \exp(-t^2/2)$. With the choice of $t_* = 2.2$ ps, $\nu = 2.2$ W$^{-1}$ km$^{-1}$, and $P_* = 1$ mW (i.e., $z_{\mathrm{NL}} = 450$ km and $k''_* = -0.01$ ps$^2$/km), the pulse has the path-average peak power of 1 mW and the FWHM of 3.7 ps (at minimum). The fiber loss is 0.2 dB/km and the amplifier period is 45 km.

In Fig. 2, we show comparison of the spectral profile of the quasi-linear pulse for $s = 50$ (corresponding to $k'' = \pm 22$ ps$^2$/km), after a propagation of $z = 20$ ($z_{\mathrm{lab}} = 9000$ km), as well as the initial profile with (a) $\zeta_a = 0$ and (b) $-1/2$. The analytical result is obtained by

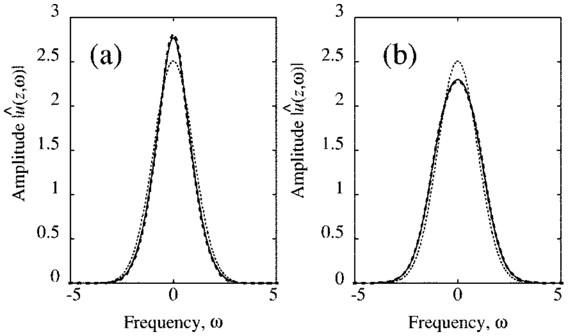


Fig. 2. The spectrum of the quasi-linear Gaussian pulse for $s = 50$. (a) $\zeta_a = 0$. (b) $\zeta_a = -1/2$. The solid curve is the pulse at $z = 20$ (i.e., 9000 km) obtained from the direct simulation, and the dashed curve shows the analytical result obtained from (5). The dotted curve is the initial profile, which is below the final profiles in (a) and above in (b).

solving (5) numerically. We see that the nonlinearity yields spectral compression and broadening when $\zeta_a = 0$ and $-1/2$, respectively. Remarkable agreement between the analysis and numerical results is obtained, which confirms the validity of our model. Since the spectral evolution is a consequence of the nonlinearity, considerable spectral reshaping may be observed by increasing the launch power. Note, however, that the nonlinearity is mitigated for large $s$, by $O(\log s/s)$ and the spectral reshaping effect is $O(1/s)$. We also note that when $\zeta_a = 0$ or $-1/2$, since the spectral reshaping is not associated with phase modulation, the observed spectral compression/broadening accompanies pulse broadening/compression, respectively, in the time domain. This implies the possibility of transform-limited temporal or spectral compression of laser pulses, once the nonlinear phase shift, which can be estimated from (5), is removed. The analysis presented here is consistent with the recent experimental and numerical observations of spectral compression of RZ pulses in strongly dispersion-managed lines [4]–[6].

Fig. 3 shows the evolution of the spectral peak amplitude $|\hat{u}(z, \omega = 0)|$ for $s = 50$, with $\zeta_a = 0$, $-1/2$, $-1/4$, and $1/4$, obtained from the direct numerical simulation and the analytical approximation (8). Since energy is conserved during propagation, the increase and decrease of the peak amplitude when $\zeta_a = 0$ and $-1/2$ demonstrates the spectral compression and broadening, respectively. On the other hand, with $\zeta_a = -1/4$ and $1/4$ the spectrum is still conserved, namely nonlinearity is responsible only for a phase shift. The deviation of the analytical approximation from the numerics for large $z$ is a consequence of the growth of the term $(K_2 z/s) f(0, \omega)$ in (8). To be valid, $(K_2 z/s) f(0, \omega)/|\hat{U}(0, 0)|^2$ should be small. We also plot a reasonable upper limit for the validity of the asymptotics (namely $z < (K_2 z/s) f(0, \omega) = 15.5$).

In conclusion, we have studied the effect of nonlinearity on quasi-linear pulse transmission. The effective nonlinearity decreases for large $s$, as $O(\log s/s)$. The periodic perturbation due to loss and lumped amplification modifies the averaged

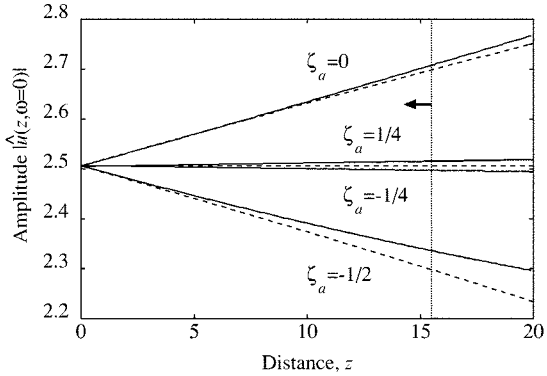


Fig. 3. The evolution of the spectral peak amplitude $|\hat{u}(z, \omega = 0)|$ for several values of $\zeta_a$. Solid lines are the results obtained from the direct simulation, and the dashed lines show the analytical approximation obtained from (8). Dotted line shows a reasonable upper limit of the validity of (8), i.e., in the direction of the arrow.

dynamics of quasi-linear transmission depending on the relative position of the lumped amplifiers. When the amplifiers are placed at the locations where the dispersion changes, the spectral intensity is found to be preserved in the evolution. Otherwise the spectral intensity varies as $O(1/s)$ and spectral compression/broadening is obtained. We have quantified the phase shift and the amount of spectral reshaping due to nonlinearity.

## References

[1] N. S. Bergano, C. R. Davidson, M. Ma, A. Pillipetskii, S. G. Evangelides, H. D. Kidorf, J. M. Darcie, E. Golovchenko, K. Rottwitt, P. C. Corbett, R. Menges, M. A. Mills, B. Pedersen, D. Peckham, A. A. Abramov, and A. M. Vengsarkar, *Dig. Optical Fiber Communications Conf.*, Washington, DC, 1998, Postdeadline Paper 12.

[2] P. Harper, S. B. Alleston, I. Bennion, and N. J. Doran, "40 Gbit/s dispersion managed soliton transmission over 1160 km in standard fiber with 75 km span length," *Electron. Lett.*, vol. 35, pp. 2128–2130, 1999.

[3] M. J. Ablowitz, T. Hirooka, and G. Biondini, "Quasilinear optical pulses in strongly dispersion-managed transmission systems," *Opt. Lett.*, vol. 26, pp. 459–461, 2001.

[4] S. Shen, C.-C. Chang, H. P. Sardesai, V. Binjrajka, and A. M. Weiner, "Effects of self-phase modulation on sub-500 fs pulse transmission over dispersion compensated fiber links," *J. Lightwave Technol.*, vol. 17, pp. 452–461, Mar. 1999.

[5] S. T. Cundiff, B. C. Collings, L. Boivin, M. C. Nuss, K. Bergman, W. H. Knox, and S. G. Evangelides Jr, "Propagation of highly chirped pulses in fiber-optic communications systems," *J. Lightwave Technol.*, vol. 17, pp. 811–816, May 1999.

[6] R.-M. Mu, T. Yu, V. S. Grigoryan, and C. R. Menyuk, "Convergence of the CRZ and DMS formats in WDM systems using dispersion management," in *Dig. Optical Fiber Communications Conf.*, Washington, DC, 2000, Paper FC1.

[7] M. J. Ablowitz and G. Biondini, "Multiscale pulse dynamics in communication systems with strong dispersion management," *Opt. Lett.*, vol. 23, pp. 1668–1670, 1998.

[8] I. R. Gabitov and S. K. Turitsyn, "Averaged pulse dynamics in a cascaded transmission system with passive dispersion compensation," *Opt. Lett.*, vol. 21, pp. 327–329, 1996.

[9] J. H. B. Nijhof, N. J. Doran, W. Forysiak, and A. Berntson, "Energy enhancement of dispersion-managed solitons and WDM," *Electron. Lett.*, vol. 34, pp. 481–482, 2000.

[10] V. E. Zakharov and S. V. Makakov, "On propagation of short pulses in strong dispersion managed optical lines," *JETP Lett*, vol. 70, pp. 578–582, 1999.